Numerical issues and turnpike phenomenon in optimal shape design

Gontran Lance, Emmanuel Trélat, Enrique Zuazua

Gontran Lance, Emmanuel Trélat*, and Enrique Zuazua

Numerical issues and turnpike phenomenon in optimal shape design

Abstract: This article follows and complements [12] where we have established the turnpike property for some optimal shape design problems.
Considering linear parabolic partial differential equations where the shapes to be optimized acts as a source term, we want to minimize a quadratic criterion. Existence of optimal shapes is proved under some appropriate assumptions. We prove and provide numerical evidence of the turnpike phenomenon for those optimal shapes, meaning that the extremal time-varying optimal solution remains essentially stationary; actually, it remains essentially close to the optimal solution of an associated static problem.

Keywords: Optimal shape design, turnpike, numerical analysis, optimal control

Introduction

This paper is devoted to studying large-time shape design problems and to providing evidence of the turnpike phenomenon, stating that the optimal time-varying design mostly stays stationary along the time interval. We complete and comment on results in [12] and we focus on the numerical solving of those large-time time-varying shape design problems, which we illustrate with a number of numerical simulations. We introduce in Section 1 the general framework and theoretical results which are then numerically illustrated along the paper. We use the relaxation method which is classical in optimal shape design. Section 2 focuses on the numerical

Gontran Lance, Emmanuel Trélat, Sorbonne Université, CNRS, Université de Paris, Inria, Laboratoire Jacques-Louis Lions (LJLL), F-75005 Paris, France, lance@ljll.math.upmc.fr, emmanuel.trelat@sorbonne-universite.fr
Enrique Zuazua, Chair in Applied Analysis, Alexander von Humboldt-Professorship, Department of Mathematics Friedrich-Alexander-Universität, Erlangen-Nürnberg, 91058 Erlangen, Germany;
Chair of Computational Mathematics, Fundación Deusto Av. de las Universidades 24, 48007 Bilbao, Basque Country, Spain;
Departamento de Matemáticas, Universidad Autónoma de Madrid, 28049 Madrid, Spain, enrique.zuazua@fau.de

implementation issues, with an approach following the theoretical study. Some numerical illustrations of the turnpike phenomenon in shape design are given in Section 3. In Section 4, we give some open questions and issues. We illustrate with numerical examples some geometric properties of optimal solutions. A section is particularly set apart for the open issue of the kinetic interpretation of shallow water equations for solving a given shape design problem. We finally provide some proofs in an appendix.

1 Optimal shape design in parabolic case

1.1 Context

Throughout the paper, we denote by:
- $|Q|$ the Lebesgue measure of a measurable subset $Q \subset \mathbf{R}^d$, $d \geq 1$;
- (p, q) the scalar product in $L^2(\Omega)$ of p, q in $L^2(\Omega)$;
- $\|y\|$ the L^2-norm of $y \in L^2(\Omega)$;
- χ_ω the indicator (or characteristic) function of $\omega \subset \mathbf{R}^d$;
- d_ω the distance function to the set $\omega \subset \mathbf{R}^d$.

Let $\Omega \subset \mathbf{R}^d$ ($d \geq 1$) be an open bounded Lipschitz domain. We consider the uniformly elliptic second-order differential operator

$$Ay = -\sum_{i,j=1}^{d} \partial_{x_j}\big(a_{ij}(x)\partial_{x_i} y\big) + \sum_{i=1}^{d} b_i(x)\partial_{x_i} y + c(x)y$$

with $a_{ij}, b_i \in C^1(\Omega)$, $c \in L^\infty(\Omega)$ with $c \geq 0$. We consider the operator $(A, D(A))$ defined on the domain $D(A)$ encoding Dirichlet conditions $y_{|\partial\Omega} = 0$; when Ω is C^2 or a convex polytop in $\mathbf{R}^2$, we have $D(A) = H_0^1(\Omega) \cap H^2(\Omega)$. The adjoint operator A^* of A, also defined on $D(A)$ with homogeneous Dirichlet conditions, is given by

$$A^* v = -\sum_{i,j=1}^{d} \partial_{x_i}\left(a_{ij}(x)\partial_{x_j} v\right) - \sum_{i=1}^{d} b_i(x)\partial_{x_i} v + \left(c - \sum_{i=1}^{d} \partial_{x_i} b_i\right) v$$

and is also uniformly elliptic, see [8, Definition Chapter 6]. The operators A and A^* do not depend on t and have a constant of ellipticity $\theta > 0$ (for A written in *non-divergence form*), i.e.:

$$\sum_{i,j=1}^{d} a_{ij}(x)\xi_i\xi_j \geq \theta|\xi|^2 \qquad \forall x \in \Omega.$$

Moreover, we assume that

$$\theta > \theta_1 \tag{1}$$

where θ_1 is the largest root of the polynomial

$$P(X) = \frac{X^2}{4\min(1, C_p)} - \|c\|_{L^\infty(\Omega)} X - \frac{\sum_{i=1}^d \|b_i\|_{L^\infty(\Omega)}}{2}$$

where C_p is the Poincaré constant of Ω. This assumption is used to ensure that an energy inequality is satisfied with constants not depending on the final time T (see Appendix A.2).

We assume throughout that the operator A satisfies the classical maximum principle (see [8, sec. 6.4]) and that

$$c^* = c - \sum_{i=1}^d \partial_{x_i} b_i \in C^2(\Omega).$$

A typical example satisfying all assumptions above is the Dirichlet-Laplacian, which we will consider in some of our numerical simulations.

We recall that the Hausdorff distance between two compact subsets K_1, K_2 of $\mathbf{R}^d$ is defined by

$$d_{\mathcal{H}}(K_1, K_2) = \sup\Big(\sup_{x\in K_2} d_{K_1}(x), \sup_{x\in K_1} d_{K_2}(x)\Big).$$

1.2 Setting

Let $L \in (0,1)$. We define the set of admissible shapes

$$\mathcal{U}_L = \{\omega \subset \Omega \text{ measurable } \mid |\omega| \le L|\Omega|\} \tag{2}$$

Dynamical optimal shape design problem ($\mathbf{DSD_T}$)
Let $y_0 \in L^2(\Omega)$ and let $\gamma_1 \ge 0, \gamma_2 \ge 0$ be arbitrary. We consider the parabolic equation controlled by a (measurable) time-varying map $t \mapsto \omega(t)$ of subdomains

$$\partial_t y + Ay = \chi_{\omega(\cdot)}, \qquad y_{|\partial\Omega} = 0, \qquad y(0) = y_0 \tag{3}$$

Given $T > 0$ and $y_d \in L^2(\Omega)$, we consider the dynamical optimal shape design problem ($\mathbf{DSD_T}$) of determining a measurable path of shapes $t \mapsto \omega(t) \in \mathcal{U}_L$ that minimizes the cost functional

$$J_T(\omega(\cdot)) = \frac{\gamma_1}{2T} \int_0^T \|y(t) - y_d\|^2 \, dt + \frac{\gamma_2}{2} \|y(T) - y_d\|^2$$

where $y = y(t,x)$ is the solution of (3) corresponding to $\omega(\cdot)$.

Static optimal shape design problem (**SSD**)
For the same target function $y_d \in L^2(\Omega)$, we consider the associated static shape design problem

$$\min_{\omega \in \mathcal{U}_L} \frac{\gamma_1}{2} \|y - y_d\|^2, \quad Ay = \chi_\omega, \quad y_{|\partial\Omega} = 0 \tag{SSD}$$

1.3 Results

1.3.1 Existence of solutions

Existence and uniqueness of solutions have been established in [12]. To facilitate the reading, we give a sketch of proof in the static case in Section A.3. In few words, we consider a relaxation of ($\mathbf{DSD_T}$) and (**SSD**) with the following idea: we replace the source term χ_ω, the characteristic function of some shape $\omega \in \mathcal{U}_L$ by a function $a \in L^\infty(\Omega, [0,1])$ (*convexification*, also called *relaxation* in classical optimal shape design theory). We can then use classical arguments of optimal control theory such as the use of the adjoint variable and the application of first-order optimality conditions coming from the Pontryagin maximum principle (see [16, Chapter 2, Theorem 1.4; Chapter 3, Theorem 2.1]). Convexification methods can be found in [2] and are a particular case of homogenization methods in shape design which are also very powerful for numerical design. In Section 2.1 we introduce the convexified (relaxed) version of the problems ($\mathbf{DSD_T}$) and (**SSD**). Existence of optimal shapes is ensured under appropriate assumptions (see [12] for complete proofs).

Theorem 1 ([12])**.** *We distinguish between Lagrange and Mayer cases.*

1. $\gamma_1 = 0, \gamma_2 = 1$ *(Mayer case): If A is analytic hypoelliptic in Ω then there exists a unique optimal shape ω_T solution of* ($\mathbf{DSD_T}$).
2. $\gamma_1 = 1, \gamma_2 = 0$ *(Lagrange case): Assuming that $y_0 \in D(A)$ and that $y_d \in H^2(\Omega)$:*
   (i) If $y_d < y^0$ or $y_d > y^1$ then there exist unique optimal shapes $\bar{\omega}$ and ω_T, respectively solutions of (**SSD**) *and of* ($\mathbf{DSD_T}$).
   (ii) There exists a function β such that if $Ay_d \leq \beta$, then there exists a unique optimal shape $\bar{\omega}$, solution of (**SSD**).

Some illustrations are provided in Section 2.2. Under the assumptions of Theorem 1, we next derive turnpike properties.

1.3.2 Turnpike

The turnpike phenomenon was first observed and investigated by economists for discrete-time optimal control problems (see [7, 17]). There are several possible notions of turnpike properties, some of them being stronger than the others (see [27]). *Exponential turnpike* properties have been established in [9, 19, 20, 23, 24, 25] for the optimal triple resulting of the application of Pontryagin's maximum principle, ensuring that the extremal solution (state, adjoint and control) remains exponentially close to an optimal solution of the corresponding static controlled problem, except at the beginning and at the end of the time interval, as soon as T is large enough. This follows from hyperbolicity properties of the Hamiltonian flow. In [12] we establish some results on turnpike property for linear parabolic optimal shape design problem. We denote by $(y_T, p_T, \chi_{\omega_T})$ and $(\bar{y}, \bar{p}, \chi_{\bar{\omega}})$ the optimal triple of both problems ($\mathbf{DSD_T}$) and (**SSD**). We show that the dynamical optimal triple, when T is large, remains most of the time "close" to the static optimal triple. In the Mayer case, we show that the Hausdorff distance between the dynamical optimal shape and the static one satisfies an exponential turnpike.

Theorem 2 ([12]). *For $\gamma_1 = 0, \gamma_2 = 1$ (Mayer case), for Ω with C^2 boundary and $c = 0$ there exist $T_0 > 0$, $M > 0$ and $\mu > 0$ such that, for every $T \geq T_0$,*

$$d_{\mathcal{H}}\big(\omega_T(t), \bar{\omega}\big) \leq M e^{-\mu(T-t)} \qquad \forall t \in (0, T).$$

Concerning the Lagrange case, an exponential turnpike property is conjectured, supported by several numerical simulations (see Section 3) but for theoretical results, we only establish integral and measure turnpike properties.

Theorem 3 ([12]). *For $\gamma_1 = 1, \gamma_2 = 0$ (Lagrange case), there exists $M > 0$ (independent of the final time T) such that*

$$\int_0^T \left(\|y_T(t) - \bar{y}\|^2 + \|p_T(t) - \bar{p}\|^2 \right) dt \leq M \qquad \forall T > 0.$$

Theorem 4 ([12]). *For $\gamma_1 = 1, \gamma_2 = 0$ (Lagrange case), the state-adjoint pair (y_T, p_T) satisfies the* state-adjoint measure-turnpike property*: for every $\varepsilon > 0$, there exists $\Lambda(\varepsilon) > 0$, independent of T, such that*

$$|P_{\varepsilon,T}| < \Lambda(\varepsilon) \qquad \forall T > 0$$

where $P_{\varepsilon,T} = \big\{ t \in [0,T] \ \mid \ \|y_T(t) - \bar{y}\| + \|p_T(t) - \bar{p}\| > \varepsilon \big\}$.

Proofs are done in [12] but, for the convenience of the reader, we give a sketch of proof of Theorem 3 in Appendix A.3. Based on the numerical simulations presented in Section 3, we conjecture that the exponential turnpike property is satisfied, i.e., given optimal triples $(y_T, p_T, \chi_{\omega_T})$ and $(\bar{y}, \bar{p}, \bar{\omega})$, there exist $C_1 > 0$ and $C_2 > 0$ independent of T such that

$$\|y_T(t) - \bar{y}\| + \|p_T(t) - \bar{p}\| + \|\chi_{\omega_T(t)} - \chi_{\bar{\omega}}\| \leq C_1 \Big(e^{-C_2 t} + e^{-C_2(T-t)} \Big)$$

for a.e. $t \in [0, T]$.

2 Numerical implementation

Computation of the cost function is conditioned to solve the PDE (3). We use a variational formulation and a finite element approach. Using **FreeFEM++** we consider a mesh of the domain Ω, a finite element space with $\mathbb{P}1$-Lagrange elements and decompose all functions according to this triangulation. To solve numerically ($\mathbf{DSD_T}$) and (**SSD**), we consider convexification method which introduces a more general problem whose solution is expected to be a shape under the assumptions of Theorem 1 and whose solution is computed via an interior point optimization method (IpOpt, see [26]).

2.1 Convexification method

The convexification method is a relaxation of the initial problem which allows to use classical tools of PDE optimal control. This is a well known method in shape optimization which has the double benefit to provide strategies to set theoretical results (see Section A.3 and see [21]) and a framework for numerical solving. Given any measurable subset $\omega \subset \Omega$, we identify ω with its indicator (characteristic) function $\chi_\omega \in L^\infty(\Omega; \{0, 1\})$ and, following [3, 21, 22], we identify $\mathcal{U}_L$ with a subset of $L^\infty(\Omega)$. Then, the convex closure of $\mathcal{U}_L$ in L^∞ weak star topology is the set

$$\overline{\mathcal{U}}_L = \left\{ a \in L^\infty\big(\Omega; [0, 1]\big) \quad \middle| \quad \int_\Omega a(x)\, dx \leq L|\Omega| \right\} \tag{4}$$

which is weak star compact. More generally, we refer the reader to [2] for details on convexification and homogenization methods. We define the *convexified* (or *relaxed*) optimal control problem $(\mathbf{OCP})_\mathbf{T}$ as the problem of determining a control

$t \mapsto a(t) \in \overline{\mathcal{U}}_L$ minimizing the cost

$$J_T(a) = \frac{\gamma_1}{2T} \int_0^T \|y(t) - y_d\|^2 \, dt + \frac{\gamma_2}{2} \|y(T) - y_d\|^2$$

under the dynamical constraints

$$\partial_t y + Ay = a, \qquad y_{|\partial\Omega} = 0, \qquad y(0) = y_0. \tag{5}$$

The corresponding convexified static optimization problem is

$$\min_{a \in \overline{\mathcal{U}}_L} \frac{\gamma_1}{2} \|y - y_d\|^2, \qquad Ay = a, \qquad y_{|\partial\Omega} = 0. \tag{SOP}$$

Solving $(\mathbf{OCP})_\mathbf{T}$ and (**SOP**) under the assumptions of Theorem 1 implies that the optimal solutions of these convexified problems happen to be the upper level sets of the adjoint-state and hence are shapes that are the optimal solutions, respectively, of $(\mathbf{DSD_T})$ and of (**SSD**). When the assumptions done in Theorem 1 are not satisfied, a relaxation phenomenon might be observed, namely, it may happen that the optimal solution of $(\mathbf{OCP})_\mathbf{T}$ or of (**SOP**) is not the characteristic function of some subset, insofar it takes values in $(0, 1)$ on a subset of positive measure. In Section 2.2 we give an example of a target function y_d such that the optimal solution $\bar{a}$ of (**SOP**) is not 0 or 1.

Since $(\mathbf{OCP})_\mathbf{T}$ and (**SOP**) are almost linear quadratic, we generate a mesh of Ω and we introduce the finite element space V_h of $\mathbb{P}1$-Lagrange element with its basis $(\omega_i) \in H^1(\Omega)$. Introducing the matrices

$$A_{ij} = \int_\Omega \nabla\omega_i \cdot \nabla\omega_j \, dx, \quad B_{ij} = \int_\Omega \omega_i\omega_j \, dx, \quad L_{v_i} = \int_\Omega \omega_i \, dx$$

we write (**SOP**) as

$$\min_{(Y,U) \in \mathbf{R}^{2N_v}} (Y - Y_d)^T B (Y - Y_d), \quad AY = BU, \quad L_v^T U \leq L|\Omega| \tag{6}$$

where N_v is the size of the finite element space (for $\mathbb{P}1$-Lagrange elements, N_v is the number of vertices). For time-discretization, we use an implicit Euler scheme with N_t steps. Introducing the matrices

$$A_t = A + \frac{1}{\delta t} B, \qquad B_t = \frac{1}{\delta t} B, \qquad \delta t = \frac{T}{N_t - 1} \tag{7}$$

$$\tilde{A} = \begin{pmatrix} I_{N_v} & 0_{N_v} & \cdots & 0_{N_v} \\ B_t & A_t & \ddots & \vdots \\ \vdots & \ddots & \ddots & 0_{N_v} \\ 0_{N_v} & \cdots & B_t & A_t \end{pmatrix}, \qquad \tilde{B} = \begin{pmatrix} 0_{N_v} & 0_{N_v} & \cdots & 0_{N_v} \\ 0_{N_v} & B_t & \ddots & \vdots \\ \vdots & \ddots & \ddots & 0_{N_v} \\ 0_{N_v} & \cdots & 0_{N_v} & B_t \end{pmatrix} \tag{8}$$

we write $(\mathbf{OCP})_{\mathbf{T}}$ as

$$\min \left\{ (Y-Y_d)^T \tilde{B}(Y-Y_d) \quad \middle| \quad (Y,U) \in \mathbf{R}^{2N_v N_t}, \quad \tilde{A}Y = \tilde{B}U, \right.$$
$$\left. L_v^T U_i \leq L|\Omega| \qquad \forall i \in \{1 \cdots N_t\} \right\} \tag{9}$$

The state variable Y is seen here as an optimization variable. The discretized convexified problems are linear quadratic optimization problems with inequality and equality constraints. It is then easy to compute the derivatives of the various functions involved. We implement them as well as their derivatives and we call the optimization routine IpOpt via **FreeFEM++**. The more information on derivatives and Hessians we give to IpOpt the faster solving is. To solve (6) and (9) we compute the gradient and Hessian of the cost function, the Jacobian of the constraint function and we add (dummy) bound variables to help the solver.

2.2 Some numerical examples

We present here some particular cases of the following optimization problem (**SSD**)

$$\min_{\omega} \frac{1}{2}\|y - y_d\|^2, \quad Ay = \chi_\omega, \quad y_{|\partial\Omega} = 0, \quad |\omega| \leq L|\Omega|$$

for some various operators A, spaces Ω and target functions y_d.

2.2.1 $\Omega = [-1,1]^2$, $y_d = 0.1$ and $A = -\triangle$

We solve here the problem for $y_d = 0.1$ and $y_d = \frac{2-x^2+y^2}{20}$. The function y_d satisfies the assumptions done in Theorem 1 in the first example and does not in the second one. Convexification method does not require many iterations. This may be due to two facts: first, IpOpt is known to be a very efficient optimization method; second, we have implemented the Hessian of the cost function and we have therefore a Newton method. We notice in the second case, when $y_d = \frac{2-x^2+y^2}{20}$ is no more convex that the optimal solution is not 0 or 1 but, in the middle of Ω, takes values into $(0,1)$.

2.2.2 $\Omega = [-1,1]^2$, $y_d = 0.1$ and A second-order operator

Here, the assumptions of Theorem 1 are not always satisfied. We take various second-order operators A, of ellipticity constant $\theta_1 > 0$, $\theta_1 = 0$ or $\theta_1 < 0$ with the following operators:

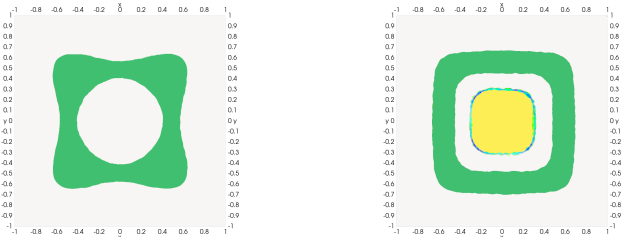

(a) (b)

Fig. 1: Optimal static shape: (a) $y_d = 0.1$; (b) $y_d = \frac{2-x^2+y^2}{20}$.

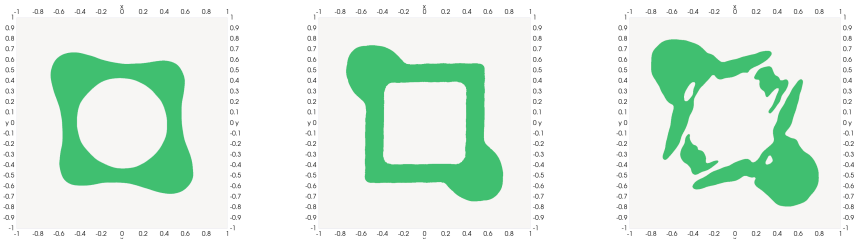

(a) (b) (c)

Fig. 2: Optimal static solution: (a) $\theta_1 > 0$; (b) $\theta_1 = 0$; (c) $\theta_1 < 0$.;

- $\theta_1 > 0 : Ay = -\partial_{11}y - \partial_{22}y - 0.5\partial_{12}y - 0.5\partial_{21}y$
- $\theta_1 = 0 : Ay = -\partial_{11}y - \partial_{22}y - \partial_{12}y - \partial_{21}y$
- $\theta_1 < 0 : Ay = -\partial_{11}y - \partial_{22}y - 1.5\partial_{12}y - 1.5\partial_{21}y$

When $\theta_1 > 0$, we are in the hypothesis of Theorem 1. When $\theta_1 = 0$, it seems we lose some regularity on the optimal solution. Finally, when $\theta_1 < 0$, we still observe convergence of our algorithm but we can no more infer the theoretical results stated at the beginning.

2.2.3 $\Omega = [-1, 1]^3$, $y_d = 0.025$ and $A = -\triangle$

FreeFEM++ is also very powerful to solve PDEs in 3D. Except mesh generation, the previously described methods are unchanged. Of course, in 3D the time required

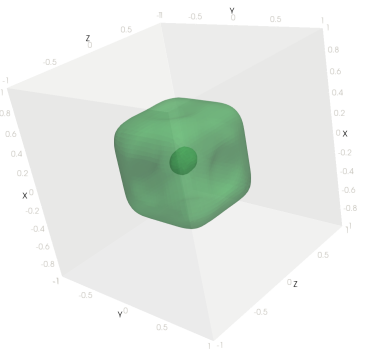

Fig. 3: Optimal static shape 3D

to compute the solution is much larger and will be a limiting factor for the solving of the time problem.

3 Numerical examples illustrating the turnpike phenomenon

In this section, in order to illustrate the turnpike phenomenon, we give numerical simulations for various domains, target functions y_d and operators A.

Case: $\Omega = [-1,1]^2$**,** $y_d = 0.1$ **and** $A = -\triangle$
We plot on Figure 4 the time solution cylinder and the shape's behavior at some sample times and for several examples. We plot in comparison the time shape at the middle-time of the trajectory and we observe that it is very similar to the optimal static shape.

To observe the exponential turnpike phenomenon we plot the quantity $t \mapsto \|y_T(t) - \bar{y}\| + \|p_T(t) - \bar{p}\| + \|\chi_{\omega_T(t)} - \chi_{\bar{\omega}}\|$ for various final times $T \in \{1, 3, 5\}$ on Figure 5.

The larger is T, the more close to 0 is the residual between the two optimal triples. The behavior of the residual function is typical of the exponential turnpike and supports our conjecture that this phenomenon might be proved. Moreover, we observe that, most of the time, the dynamical shape remains very close to the static one. These numerical observations seem to hold systematically under the assumptions done in Theorem 1. The turnpike phenomenon occurs even when we observe relaxation or when the second-order operator A is such that $\theta_1 = 0$.

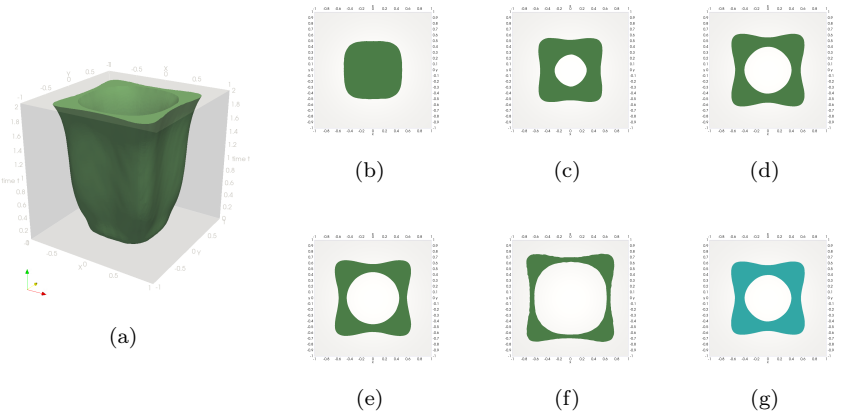

Fig. 4: Optimal dynamical shape: (a) Time shape; (b) $t = 0$; (c) $t = 0.5$; (c) $t \in (0.5, 1.5)$; (e) $t = 1.5$; (f) $t = T$; (g) Static shape.

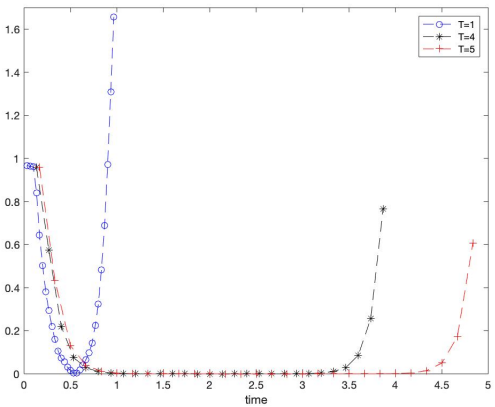

Fig. 5: $t \mapsto \|y_T(t) - \bar{y}\| + \|p_T(t) - \bar{p}\| + \|\chi_{\omega_T(t)} - \chi_{\bar{\omega}}\|$ for $T \in \{1, 3, 5\}$

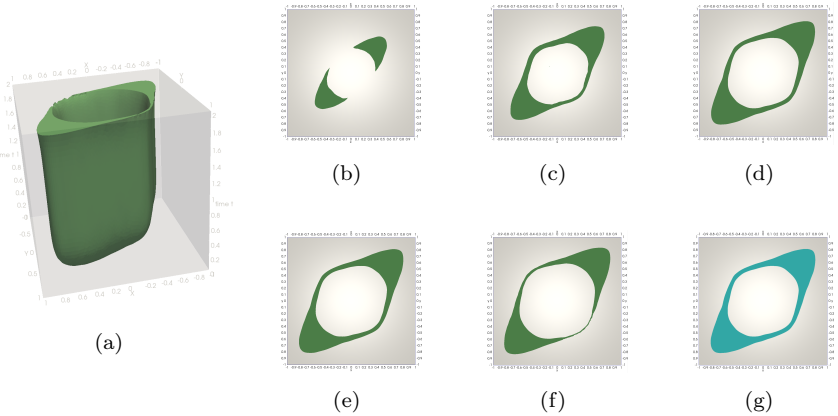

(a) (b) (c) (d) (e) (f) (g)

Fig. 6: (a) Time shape; (b) $t = 0$; (c) $t = 0.5$; (c) $t \in (0.5, 1.5)$; (e) $t = 1.5$; (f) $t = T$; (g) Static shape.

Case: $\Omega = [-1, 1]^2$**,** $y_d = \frac{1}{20}(xy + 1)$ **and** $A = -\triangle$
Case: $\Omega =$ **half-stadium,** $y_d = \frac{1}{20}(xy + 1)$ **and** $A = -\triangle$
Case: $\Omega = [-1, 1]^2$**,** $y_d = \frac{1}{20}(2\sin(2(x^2 + y^2)) + 1)$ **and** $Au = -\partial_x((x - y)^2\partial_x u) - \partial_y((x + y)^2\partial_y u)$
Case: $\Omega = [-1, 1]^3$**,** $y_d = 0.025$ **and** $Au = -\triangle$

4 Further comments

We highlight here some open questions and possible way to pursue the research. Some geometric properties can be conjectured and we address the question of shape design for semi-linear partial differential equations. Finally, we present shortly a shape design problem in the context of shallow water equations.

4.1 Symmetries of solutions

On the basis of our numerical examples, we conjecture that if Ω, the operator A and the target function y_d share the same symmetry properties, then optimal solutions $\bar{\omega}$ and $\omega_T(\cdot)$ share as well symmetry properties.

For instance, Figure 10(a) highlights four axes of symmetry ($x = 0, y = 0, y = x, y = -x$), Figure 10(b) two axes ($y = x, y = -x$) and Figure 10(c) shows up a central symmetry property (of center $(0, 0)$ and with angle π).

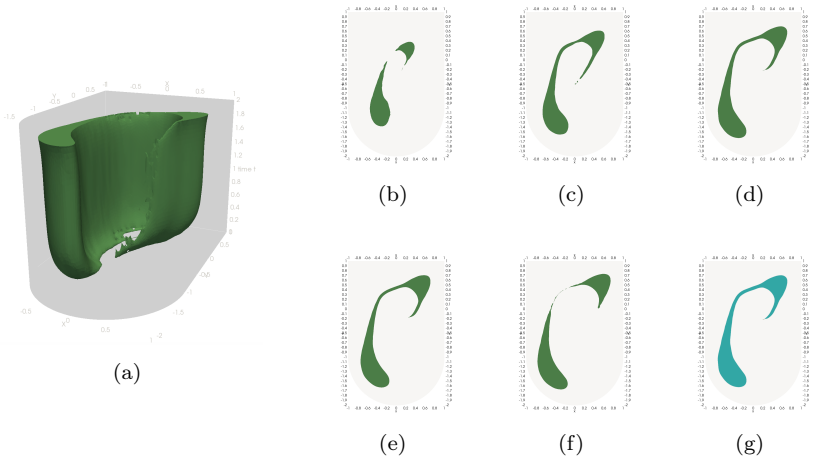

Fig. 7: (a) Time shape; (b) $t = 0$; (c) $t = 0.5$; (c) $t \in (0.5, 1.5)$; (e) $t = 1.5$; (f) $t = T$; (g) Static shape.

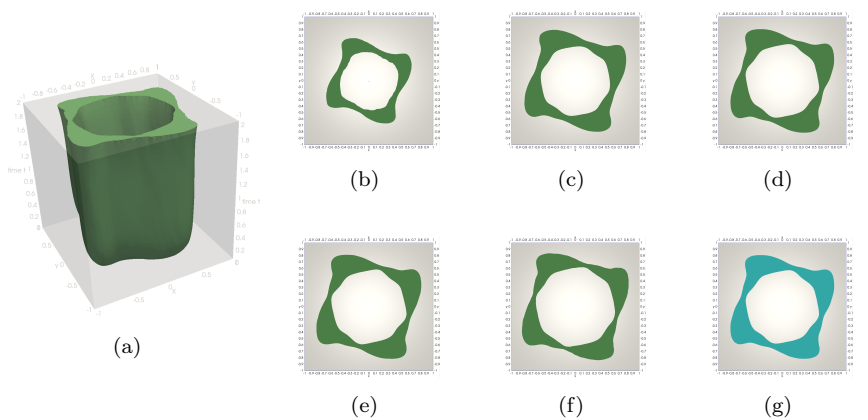

Fig. 8: (a) Time shape; (b) $t = 0$; (c) $t = 0.5$; (c) $t \in (0.5, 1.5)$; (e) $t = 1.5$; (f) $t = T$; (g) Static shape.

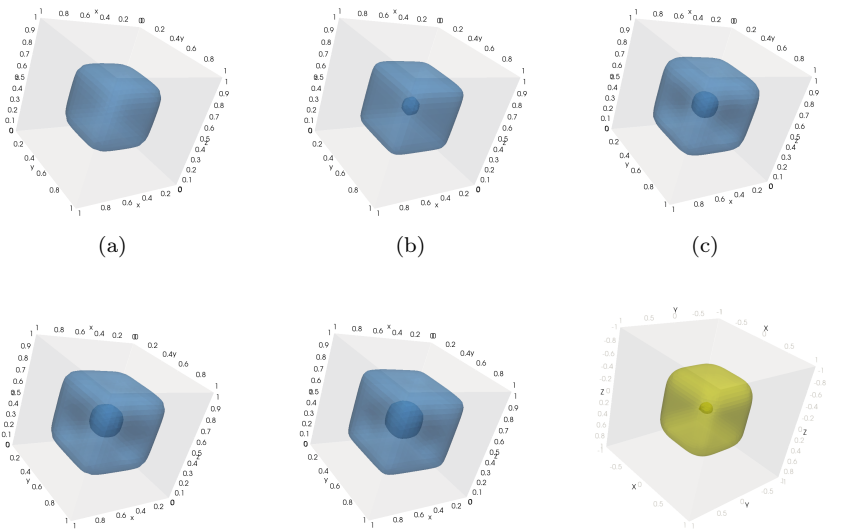

(a) (b) (c)

(d) (e) (f)

Fig. 9: Time shape: (a) $t = 0$; (b) $t = 0.1$; (b) $t \in]0.1, 0.9[$; (d) $t = 0.9$; (e) $t = T = 1$; (f) Static shape.

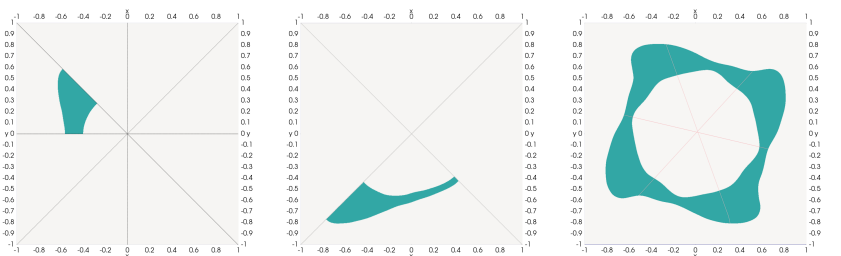

(a) (b) (c)

Fig. 10: Symmetries of static optimal shapes : (a) $A = -\triangle, y_d = 0.1$; (b) $A = -\triangle, y_d = \frac{xy+1}{20}$; (c) $Au = -\partial_x((x-y)^2\partial_x u) - \partial_y((x+y)^2\partial_y u), y_d = \frac{1}{20}(2\sin(2(x^2+y^2)) + 1)$

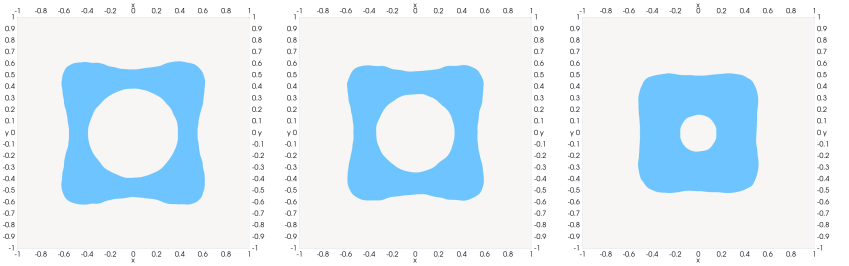

(a) (b) (c)

Fig. 11: Semilinear static optimal designs : (a) $f(y) = y(1-y^2)\exp(y)\sin(y)$; (b) $f(y) = (y+0.4)^3$; (c) $f(y) = \frac{1}{y+5}$.

4.2 Semilinear PDEs and numerics

An open and interesting issue is to deal with semilinear PDEs

$$\partial_t y + Ay + f(y) = \chi_\omega, \quad y_{|\partial\Omega} = 0, \quad y(0) = y_0.$$

Theoretical results are not established in this context but we refer to [10] where authors are interested in semilinear shape optimization problems and whose existence proofs involve shape optimization problems close to the one we deal with in this section. From our side, we provide hereafter several first numerical simulations. We still use the convexification approach combining IpOpt and **FreeFEM++** for numerical solving. Now, anyway, systems cannot be written as linear quadratic optimization problem as (6) and (9). We use a fixed point method, so that the solution of the static problem

$$Ay + f(y) = \chi_\omega, \quad y_{|\partial\Omega} = 0 \tag{10}$$

is sought with an iteration process.

We show on Figure 11 some examples of solutions for several functions f and for $A = -\triangle$.

We observe that the optimal solutions are quite similar to the solutions obtained in the linear case. For theoretical results, due to the nonlinearity, new assumptions should be made in order to ensure existence and/or uniqueness of solutions. We still observe the turnpike phenomenon for the optimal shape design in 1D. We take $\Omega = [0,2], A = -\triangle, y_d = 0.1$ and $T = 10$. We plot on Figure 12 the dynamical optimal shape and we observe that it remains most of the time stationary (which is the solution of the corresponding static optimal shape problem). Moreover, we plot the error between both optimal triples and we still observe an exponential turnpike phenomenon.

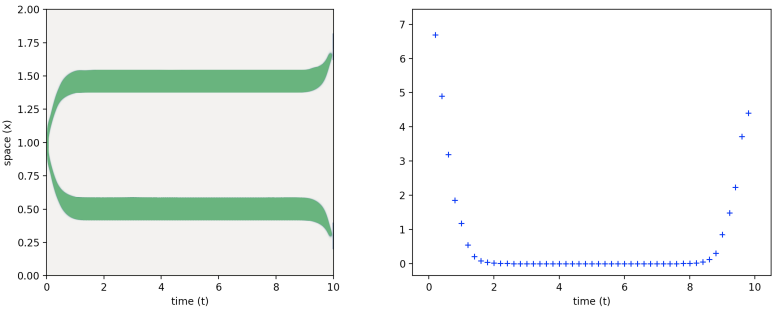

(a) (b)

Fig. 12: Semilinear optimal designs: (a) Dynamical optimal shape; (b) $t \mapsto \|y_T(t) - \bar{y}\| + \|p_T(t) - \bar{p}\| + \|\chi_{\omega_T)(t)} - \chi_{\bar{\omega}}\|$.

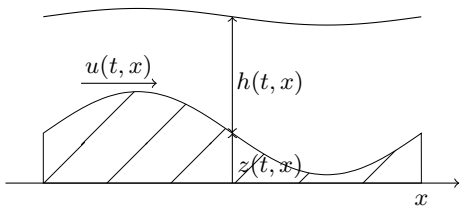

Fig. 13: Shallow water equations

4.3 Optimal design for shallow water equations

4.3.1 Presentation

We consider the shallow water system in space dimension one, a specific case of shallow water equations, which is a usual way to understand the behavior of a fluid when the height of the water level is much smaller than the other spatial dimensions of the problem, for instance flows in river or in maritime coast. Using several assumptions (small height of water, hydrostatic pressure, vertical homogeneity of horizontal velocities, etc), we can derive these from the Euler system. We describe the behavior of the fluid at time $t > 0$ and at a position $x \in \mathbf{R}$ characterized by the water level $h(t,x)$ and the flow $h(t,x)u(t,x)$ and we take into account the variation of the topography $z(t,x)$ and some viscous effects S_f. We consider the bottom shape z as the control. For $T > 0$, (h_0, u_0) initial conditions and (h_d, u_d) given as a static wave profile, we search an optimal solution

minimizing the functional

$$J_{SW}(z) = \frac{1}{2}\int_0^T \|h(t) - h_d\|^2 + \|u(t) - u_d\|^2 \, dt \tag{11}$$

subject to the shallow water equations

$$\begin{aligned} &\partial_t h + \partial_x(hu) = 0 \\ &\partial_t(hu) + \partial_x(hu^2 + g\tfrac{h^2}{2}) = -gh\partial_x z + S_f \\ &h(0) = h_0, \quad u(0) = u_0 \end{aligned} \tag{12}$$

Since the target (h_d, u_d) is static, having in mind the phenomenon of static wave occuring in the nature (Eisbach Wave in München or wavemaker in [1]), we would expect that a solution, if it exists, should remain most of the time close to a stationary state solution of a static problem.

4.3.2 Kinetic interpretation of shallow water equations

To lead this study, we propose a relaxation of the problem via *kinetic equations* (see [5, 6, 18]. We consider a real-valued function χ of class C^1, compactly supported on $\mathbf{R}$, such that

$$\chi(\omega) = \chi(-\omega), \quad \int_{\mathbf{R}} \chi(\omega)\, d\omega = 1, \quad \int_{\mathbf{R}} \omega^2 \chi(\omega)\, d\omega = \frac{g^2}{2}.$$

Defining $c = \sqrt{\frac{gh}{2}}$ and

$$M(t,x,\xi) = \frac{h(t,x)}{c(t,x)}\chi\Big(\frac{\xi - u(t,x)}{c(t,x)}\Big) = \frac{h(t,x)}{c(t,x)}\chi\Big(\frac{\xi - q(t,x)}{h(t,x)c(t,x)}\Big) \tag{13}$$

we get

$$\begin{pmatrix} h \\ q \\ \frac{g}{2}h^2 + \frac{q^2}{h} \end{pmatrix} = \int_{\mathbf{R}} \begin{pmatrix} 1 \\ \xi \\ \xi^2 \end{pmatrix} M(\xi)\, d\xi. \tag{14}$$

Following [18], (h, u) is a weak solution of (12) if and only if M (defined by (13)) satisfies

$$M_t + \xi . M_x - g z_x . M_\xi = Q \tag{15}$$

for some Q, a collision factor such that $\int_{\mathbf{R}} Q\, d\xi = \int_{\mathbf{R}} \xi Q\, d\xi = 0$.

An open question is to write the initial problem as the minimization of some cost functional

$$\min_z \frac{1}{2} \int_0^T \int_{\mathbf{R}\times\Omega} f^0\big(x,\xi,M(t,x,\xi)\big)\, d\xi\, dx\, dt$$

with respect to the kinetic equations

$$M_t + \xi.M_x - g z_x.M_\xi = Q, \quad M(0) = \frac{h_0}{c_0}\chi\Big(\frac{\xi - u_0}{c_0}\Big) \tag{16}$$

This would have the double benefit to obtain in an easier way theoretical and numerical results since the nonlinear system (12) is replaced by the linear kinetic equation (15).

A Appendix

A.1 Optimality conditions

In order to show some theoretical results introduced before and in the framework provided by the convexification (see Section 2.1) we first give necessary optimality conditions to optimal solutions of the convexified problems stated in [16, Chapters 2 and 3] or [14, Chapter 4] and infer from these necessary conditions that, under appropriate assumptions, the optimal controls are indeed characteristic functions.

Necessary optimality conditions for $(\mathbf{OCP})_\mathbf{T}$

According to the Pontryagin maximum principle (see [16, Chapter 3, Theorem 2.1], see also [14]), for any optimal solution (y_T, a_T) of $(\mathbf{OCP})_\mathbf{T}$ there exists an adjoint state $p_T \in L^2(0,T;\Omega)$ such that

$$\begin{aligned} \partial_t y_T + A y_T = a_T,\ y_{T_{|\partial\Omega}} = 0,\ y_T(0) = y_0 \\ \partial_t p_T - A^* p_T = \gamma_1(y_T - y_d),\ p_{T_{|\partial\Omega}} = 0,\ p_T(T) = \gamma_2\big(y_T(T) - y_d\big) \end{aligned} \tag{17}$$

$$\forall a \in \overline{\mathcal{U}}_L, \text{for a.e. } t \in [0,T]: \quad \big(p_T(t), a_T(t) - a\big) \geq 0. \tag{18}$$

Necessary optimality conditions for (SOP)

Similarly, applying [16, Chapter 2, Theorem 1.4], for any optimal solution $(\bar{y}, \bar{a})$ of (**SOP**) there exists an adjoint state $\bar{p} \in L^2(\Omega)$ such that

$$\begin{aligned} A\bar{y} = \bar{a}, \qquad & \bar{y}_{|\partial\Omega} = 0 \\ -A^*\bar{p} = \gamma_1(\bar{y} - y_d), \qquad & \bar{p}_{|\partial\Omega} = 0 \end{aligned} \tag{19}$$

$$\forall a \in \overline{\mathcal{U}}_L : \quad (\bar{p}, \bar{a} - a) \geq 0. \tag{20}$$

Using the bathtub principle (see, e.g., [15, Theorem 1.14]), (18) and (20) give

$$a_T(\cdot) = \chi_{\{p_T(\cdot) > s_T(\cdot)\}} + c_T(\cdot)\chi_{\{p_T(\cdot) = s_T(\cdot)\}} \tag{21}$$

$$\bar{a} = \chi_{\{\bar{p} > \bar{s}\}} + \bar{c}\chi_{\{\bar{p} = \bar{s}\}} \tag{22}$$

with, for a.e. $t \in [0, T]$,

$$c_T(t) \in L^\infty(\Omega; [0,1]) \text{ and } \bar{c} \in L^\infty(\Omega; [0,1]) \tag{23}$$

$$s_T(\cdot) = \inf\left\{\sigma \in \mathbf{R} \;\middle|\; |\{p_T(\cdot) > \sigma\}| \leq L|\Omega|\right\} \tag{24}$$

$$\bar{s} = \inf\left\{\sigma \in \mathbf{R} \;\middle|\; |\{\bar{p} > \sigma\}| \leq L|\Omega|\right\}. \tag{25}$$

A.2 Energy inequalities

We recall some useful inequalities to study existence and turnpike. Since θ satisfies (1), we can find $\beta > 0, \gamma \geq 0$ such that $\beta \geq \gamma$ and

$$(Au, u) \geq \beta \|u\|^2_{H^1_0(\Omega)} - \gamma \|u\|^2_{L^2(\Omega)}. \tag{26}$$

From this follows the energy inequality (see [8, Chapter 7, Theorem 2]): there exists $C > 0$ such that, for any solution y of (5), for almost every $t \in [0, T]$,

$$\|y(t)\|^2 + \int_0^t \|y(s)\|^2_{H^1_0(\Omega)}\, ds \leq C\left(\|y_0\|^2 + \int_0^t \|a(s)\|^2\, ds\right). \tag{27}$$

Let us improve this inequality. Having in mind (26), the Poincaré inequality and that y verifies (5), we find two constants $C_1, C_2 > 0$ such that $\frac{d}{dt}\|y(t)\|^2 + C_1\|y(t)\|^2 = f(t) \leq C_2\|a(t)\|^2$. We solve this differential equation to get $\|y(t)\|^2 = \|y_0\|^2 e^{-C_1 t} + \int_0^t e^{-C_1(t-s)} f(s)\, ds$. Since for all $t \in (0, T)$, $f(t) \leq C_2\|a(t)\|^2$, we obtain that

$$\|y(t)\|^2 \leq \|y_0\|^2 e^{-C_1 t} + C_2 \int_0^t e^{-C_1(t-s)} \|a(s)\|^2\, ds \tag{28}$$

for almost every $t \in (0, T)$. The constants C, C_1, C_2 depend only on the domain Ω (Poincaré inequality) and on the operator A but not on final time T since (26) is satisfied with $\beta \geq \gamma$.

A.3 Proofs

A.3.1 Proof of Theorem 1

Here we first establish existence of optimal solutions for $(\mathbf{OCP})_{\mathbf{T}}$ and similarly for (**SOP**). Then we focus on the static case in order to highlight a key observation to derive existence of an optimal shape for (**SSD**) as well as the relaxation phenomenon.

We first see that the infimum exists. Let us take a minimizing sequence

$$(y_n, a_n) \in L^2(0,T;H_0^1(\Omega)) \times L^\infty\big(0,T;L^2\big(\Omega,[0,1]\big)\big)$$

such that, for $n \in \mathbf{N}$, for *a.e.* $t \in [0,T]$, $a_n(t) \in \overline{\mathcal{U}}_L$, the pair (y_n, a_n) satisfies (5) and $J_T(a_n) \to J_T$. The sequence (a_n) is bounded in $L^\infty\big(0,T;L^2\big(\Omega,[0,1]\big)\big)$, so using (27) and (28), the sequence (y_n) is bounded in $L^\infty(0,T;L^2(\Omega)) \cap L^2(0,T;H_0^1(\Omega))$. We show then, using (5), that the sequence $(\frac{\partial y_n}{\partial t})$ is bounded in $L^2(0,T;H^{-1}(\Omega))$. We subtract a sequence still denoted by (y_n, a_n) such that one can find a pair $(y,a) \in L^2(0,T;H_0^1(\Omega)) \times L^\infty\big(0,T;L^2\big(\Omega,[0,1]\big)\big)$ with

$$\begin{aligned} y_n &\rightharpoonup y && \text{weakly in } L^2(0,T;H_0^1(\Omega)) \\ \partial_t y_n &\rightharpoonup \partial_t y && \text{weakly in } L^2(0,T;H^{-1}(\Omega)) \\ a_n &\rightharpoonup a && \text{weakly * in } L^\infty\big(0,T;L^2\big(\Omega,[0,1]\big)\big). \end{aligned} \tag{29}$$

We deduce that

$$\begin{aligned} \partial_t y_n + A y_n - a_n &\to \partial_t y + A y - a \quad \text{in } \mathcal{D}'\big((0,T)\times\Omega\big) \\ y_n(0) &\rightharpoonup y(0) \quad \text{weakly in } L^2(\Omega). \end{aligned} \tag{30}$$

We get using (30) that (y,a) is a weak solution of (5). Moreover, since

$$L^\infty\big(0,T;L^2\big(\Omega,[0,1]\big)\big) = \Big(L^1\big(0,T;L^2\big(\Omega,[0,1]\big)\big)\Big)'$$

(see [11, Corollary 1.3.22]) the convergence (29) implies that for every $v \in L^1(0,T)$ satisfying $v \geq 0$ and $\|v\|_{L^1(0,T)} = 1$, we have

$$\int_0^T \Big(\int_\Omega a(t,x)\,dx \Big) v(t)\,dt \leq L|\Omega|.$$

Since the function f_a defined by

$$f_a(t) = \int_\Omega a(t,x)\,dx$$

belongs to $L^\infty(0,T)$, we have

$$\|f_a\|_{L^\infty(0,T)} = \sup\left\{ \int_0^T \Big(\int_\Omega a(t,x)\,dx \Big) v(t)\,dt \;\Big|\; v \in L^1(0,T),\ \|v\|_{L^1(0,T)} = 1 \right\}$$

Therefore $\|f_a\|_{L^\infty(0,T)} \leq L|\Omega|$ and $\int_\Omega a(t,x)\,dx \leq L|\Omega|$ for a.e. $t \in (0,T)$. This shows that the pair (y,a) is admissible. Since $H_0^1(\Omega)$ is compactly embedded in $L^2(\Omega)$ and by using the Aubin-Lions compactness Lemma (see [4]), we obtain

$$y_n \to y \quad \text{strongly in } L^2(0,T;L^2(\Omega)).$$

We get then by weak lower semi-continuity of J_T and by Fatou Lemma that

$$J_T(a) \leq \liminf J_T(a_n).$$

Hence a is an optimal control for $(\mathbf{OCP})_\mathbf{T}$, that we rather denote by a_T (and $\bar{a}$ for (**SOP**)).

Let us now focus on the part 2-(ii) of Theorem 1. We focus on $\gamma_1 = 1, \gamma_2 = 0$ (Lagrange case) and (**SSD**). Since $\bar{a}$ is a s solution of (**SOP**), it verifies the optimality conditions stated in (19)-(22). One key observation is to note that, if $|\{\bar{p} = \bar{s}\}| = 0$, then it follows from (22) that the static optimal control $\bar{a}$ is actually the characteristic function of a shape $\bar{\omega} \in \mathcal{U}_L$. With this in mind, we give a useful lemma.

Lemma 5 ([13, Theorem 3.2])**.** *Given any $p \in [1,+\infty)$ and any $u \in W^{1,p}(\Omega)$ such that $|\{u=0\}| > 0$, we have $\nabla u = 0$ a.e. on $\{u=0\}$.*

2-(ii) We assume that $Ay_d \leq \beta$ in Ω with $\beta = \bar{s}Ac^*$. Having in mind (19) and (22), we assume by contradiction that $|\{\bar{p} = \bar{s}\}| > 0$. Since A and A^* are differential operators, applying A^* to $\bar{p}$ on $\{\bar{p} = \bar{s}\}$, we obtain by Lemma 5 that

$$A^*\bar{p} = c^*\bar{s} \quad \text{on} \quad \{\bar{p} = \bar{s}\}.$$

Since $(\bar{y}, \bar{p})$ verifies (19) we get

$$y_d - \bar{y} = c^*\bar{s} \quad \text{on} \quad \{\bar{p} = \bar{s}\}.$$

We apply then A to this equation to get that

$$Ay_d - \bar{s}Ac^* = A\bar{y} = \bar{a} \quad \text{on} \quad \{\bar{p} = \bar{s}\}.$$

Therefore

$$Ay_d - \bar{s}Ac^* \in (0,1) \quad \text{on} \quad \{\bar{p} = \bar{s}\}$$

which contradicts $Ay_d \leq \beta$. Hence $|\{\bar{p} = \bar{s}\}| = 0$ and thus (22) implies $\bar{a} = \chi_{\bar{\omega}}$ for some $\bar{\omega} \in \mathcal{U}_L$. Existence of solution for (**SSD**) is proved.

Uniqueness of optimal controls comes from the strict convexity of the cost functionals. Indeed, in the dynamical case, whatever $(\gamma_1, \gamma_2) \neq (0, 0)$ may be, J_T is strictly convex with respect to variable y. The injectivity of the control-to-state mapping gives the strict convexity with respect to the variable a. In addition, uniqueness of $(\bar{y}, \bar{p})$ follows by application of the Poincaré inequality and uniqueness of (y_T, p_T) follows from Gronwall inequality (28) in the appendix.

Remark 6. *Condition in Theorem 1: 2-(ii) is a necessary condition. We can construct example, where $Ay_d \leq \beta$ is not satisfied and where we observe relaxation, which is closely related to the fact $|\{\bar{p} = \bar{s}\}| > 0$.*

Indeed, we plot on Figure 14 the adjoint state $\bar{p}$ for the static problem in 1D. At the left-hand side, $\bar{p}$ is assumed to be analytic: in this case, all level sets of $\bar{p}$ have zero Lebesgue measure (there is no subset of positive measure on which $\bar{p}$ would remain constant). When $\bar{p}$ is not analytic and remains constant on a subset of positive measure (see Figure 14 in red), we do not have necessarily zero Lebesgue measure level sets, and on $\{\bar{p} = \bar{s}\}$, $\bar{a}$ can take values in $(0, 1)$.

Proof of Theorem 3

For $\gamma_1 = 1, \gamma_2 = 0$ (Lagrange case), the cost is

$$J_T(\omega) = \frac{1}{2T} \int_0^T \|y(t) - y_d\|^2 \, dt.$$

We consider the triples $(y_T, p_T, \chi_{\omega_T})$ and $(\bar{y}, \bar{p}, \chi_{\bar{\omega}})$ satisfying the optimality conditions (17) and (19). Since $\chi_{\omega_T(t)}$ is bounded at each time $t \in [0, T]$ and by application of Gronwall inequality (28) in the appendix to y_T and p_T we can find a constant $C > 0$ depending only on A, y_0, y_d, Ω, L such that

$$\forall T > 0 \quad \|y_T(T)\|^2 \leq C \quad \text{and} \quad \|p_T(0)\|^2 \leq C.$$

Setting $\tilde{y} = y_T - \bar{y}, \tilde{p} = p_T - \bar{p}, \tilde{a} = \chi_{\omega_T} - \chi_{\bar{\omega}}$, we have

$$\partial_t \tilde{y} + A\tilde{y} = \tilde{a}, \quad \tilde{y}_{|\partial\Omega} = 0, \quad \tilde{y}(0) = y_0 - \bar{y} \tag{31}$$

$$\partial_t \tilde{p} - A^* \tilde{p} = \tilde{y}, \quad \tilde{p}_{|\partial\Omega} = 0, \quad \tilde{p}(T) = -\bar{p}. \tag{32}$$

First, using (17) and (19) one has $\big(\tilde{p}(t), \tilde{a}(t)\big) \geq 0$ for almost every $t \in [0, T]$. Multiplying (31) by $\tilde{p}$, (32) by $\tilde{y}$ and then adding them, one can use the fact that

$$\big(\bar{y} - y_0, \tilde{p}(0)\big) - \big(\tilde{y}(T), \bar{p}\big) = \int_0^T \big(\tilde{p}(t), \tilde{a}(t)\big) \, dt + \int_0^T \|\tilde{y}(t)\|^2 \, dt.$$

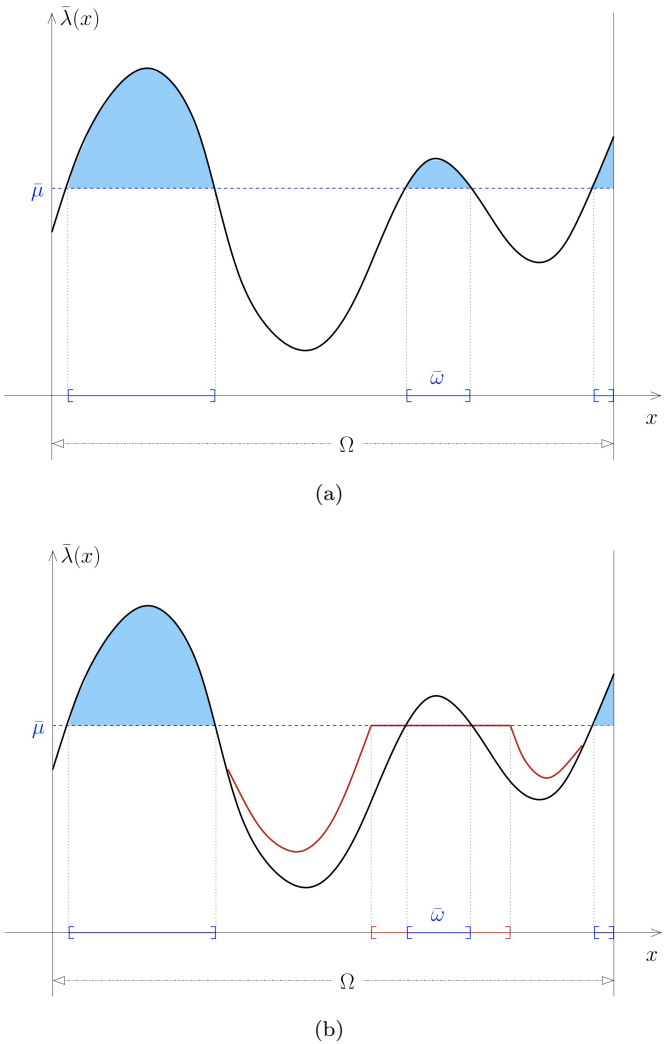

Fig. 14: Optimal shape design existence and relaxation: (a) No relaxation: Shape existence; (b) Relaxation.

By the Cauchy-Schwarz inequality we get a new constant $C > 0$ such that

$$\frac{1}{T}\int_0^T \|\tilde{y}(t)\|^2\,dt + \frac{1}{T}\int_0^T \big(\tilde{p}(t),\tilde{a}(t)\big)\,dt \le \frac{C}{T}.$$

The two terms at the left-hand side are positive and using the inequality (27) with $\zeta(t) = \tilde{p}(T-t)$, we finally obtain $M > 0$ independent of T such that

$$\frac{1}{T}\int_0^T \big(\|y_T(t)-\bar{y}\|^2 + \|p_T(t)-\bar{p}\|^2\big)\,dt \le \frac{M}{T}.$$

Acknowledgment: This project has received funding from the Grants ICON-ANR-16-ACHN-0014 and Finite4SoS ANR-15-CE23-0007-01 of the French ANR, the European Research Council (ERC) under the European Union's Horizon 2020 research and innovation programme (grant agreement 694126-DyCon), the Alexander von Humboldt-Professorship program, the Air Force Office of Scientific Research under Award NO: FA9550-18-1-0242, Grant MTM2017-92996-C2-1-R COSNET of MINECO (Spain) and by the ELKARTEK project KK-2018/00083 ROAD2DC of the Basque Government, Transregio 154 Project *Mathematical Modelling, Simulation and Optimization using the Example of Gas Networks* of the German DFG, the European Union Horizon 2020 research and innovation programme under the Marie Sklodowska-Curie grant agreement 765579-ConFlex.

References

[1] Citywave : https://citywave.de/fr/.

[2] G. Allaire. *Conception optimale de structures*, volume 58 of *Mathématiques & Applications (Berlin) [Mathematics & Applications]*. Springer-Verlag, Berlin, 2007. With the collaboration of Marc Schoenauer (INRIA) in the writing of Chapter 8.

[3] G. Allaire, A. Münch, and F. Periago. Long time behavior of a two-phase optimal design for the heat equation. *SIAM J. Control Optim.*, 48(8):5333–5356, 2010.

[4] J. Aubin. Un théorème de compacité. *C. R. Acad. Sci. Paris*, 256:5042 – 5044, 1963.

[5] E. Audusse, F. Bouchut, M.-O. Bristeau, and J. Sainte-Marie. Kinetic entropy inequality and hydrostatic reconstruction scheme for the Saint-Venant system. *Math. Comp.*, 85(302):2815–2837, 2016.

[6] M.-O. Bristeau and B. Coussin. Boundary Conditions for the Shallow Water Equations solved by Kinetic Schemes. Research Report RR-4282, INRIA, 2001. Projet M3N.

[7] R. Dorfman, P. A. Samuelson, and R. M. Solow. *Linear programming and economic analysis*. A Rand Corporation Research Study. McGraw-Hill Book Co., Inc., New York-Toronto-London, 1958.

[8] L. C. Evans. *Partial differential equations*, volume 19 of *Graduate Studies in Mathematics*. American Mathematical Society, Providence, RI, second edition, 2010.

[9] L. Grüne, M. Schaller, and A. Schiela. Exponential sensitivity and turnpike analysis for linear quadratic optimal control of general evolution equations, Dezember 2018.

[10] A. Henrot, I. Mazari, and Y. Privat. Shape optimization of a Dirichlet type energy for semilinear elliptic partial differential equations. working paper or preprint, Apr. 2020.

[11] T. Hytönen, J. van Neerven, M. Veraar, and L. Weis. *Analysis in Banach spaces. Vol. I. Martingales and Littlewood-Paley theory*, volume 63 of *Ergebnisse der Mathematik und ihrer Grenzgebiete. 3. Folge. A Series of Modern Surveys in Mathematics [Results in Mathematics and Related Areas. 3rd Series. A Series of Modern Surveys in Mathematics]*. Springer, Cham, 2016.

[12] G. Lance, E. Trélat, and E. Zuazua. Shape turnpike for linear parabolic PDE models. *Systems & Control Letters*, 142:104733,9, 2020.

[13] H. Le Dret. *Nonlinear elliptic partial differential equations*. Universitext. Springer, Cham, 2018. An introduction, Translated from the 2013 French edition [MR3235838].

[14] X. J. Li and J. M. Yong. *Optimal control theory for infinite-dimensional systems*. Systems & Control: Foundations & Applications. Birkhäuser Boston, Inc., Boston, MA, 1995.

[15] E. H. Lieb and M. Loss. *Analysis*, volume 14 of *Graduate Studies in Mathematics*. American Mathematical Society, Providence, RI, second edition, 2001.

[16] J.-L. Lions. *Optimal control of systems governed by partial differential equations*. Translated from the French by S. K. Mitter. Die Grundlehren der mathematischen Wissenschaften, Band 170. Springer-Verlag, New York-Berlin, 1971.

[17] L. W. McKenzie. Turnpike theorems for a generalized leontief model. *Econometrica*, 31(1/2):165–180, 1963.

[18] B. Perthame and C. Simeoni. A kinetic scheme for the Saint-Venant system with a source term. *Calcolo*, 38(4):201–231, 2001.

[19] A. Porretta and E. Zuazua. Long time versus steady state optimal control. *SIAM J. Control Optim.*, 51(6):4242–4273, 2013.

[20] A. Porretta and E. Zuazua. Remarks on long time versus steady state optimal control. In *Mathematical paradigms of climate science*, volume 15 of *Springer INdAM Ser.*, pages 67–89. Springer, [Cham], 2016.

[21] Y. Privat, E. Trélat, and E. Zuazua. Optimal shape and location of sensors for parabolic equations with random initial data. *Arch. Ration. Mech. Anal.*, 216(3):921–981, 2015.

[22] Y. Privat, E. Trélat, and E. Zuazua. Optimal observability of the multi-dimensional wave and Schrödinger equations in quantum ergodic domains. *J. Eur. Math. Soc. (JEMS)*, 18(5):1043–1111, 2016.

[23] E. Trélat and C. Zhang. Integral and measure-turnpike properties for infinite-dimensional optimal control systems. *Math. Control Signals Systems*, 30(1):Art. 3, 34, 2018.

[24] E. Trélat, C. Zhang, and E. Zuazua. Steady-state and periodic exponential turnpike property for optimal control problems in Hilbert spaces. *SIAM J. Control Optim.*, 56(2):1222–1252, 2018.

[25] E. Trélat and E. Zuazua. The turnpike property in finite-dimensional nonlinear optimal control. *J. Differential Equations*, 258(1):81–114, 2015.

[26] A. Wächter and L.-T. Biegler. On the Implementation of a Primal-Dual Interior Point Filter Line Search Algorithm for Large-Scale Nonlinear Programming. *Mathematical Programming 106(1), pp. 25-57*, 2006.

[27] A. J. Zaslavski. *Turnpike theory of continuous-time linear optimal control problems*, volume 104 of *Springer Optimization and Its Applications*. Springer, Cham, 2015.